

Review
**A Review of Particle- and Fiber-
Reinforced Metakaolin-Based Geopolymer Composites**

R.A. Sá Ribeiro^{*1, 2}, M.G. Sá Ribeiro², W.M. Kriven¹

¹Department of Materials Science and Engineering,
University of Illinois at Urbana-Champaign, Urbana, IL, 61801 USA

²Structural Engineering Laboratory, National Institute for
Amazonian Research, Manaus, AM, 69067–375 Brazil

received July 1, 2017; received in revised form August 7, 2017; accepted August 22, 2017

Abstract

Research on reinforced metakaolin-based geopolymers for structural applications is reviewed. Geopolymers have been synthesized using metakaolin produced from kaolinite extracted from several regional soils. Kaolin is converted into metakaolin by calcination from 650 °C up to 800 °C. To obtain higher strength and stiffness, the geopolymer matrix is reinforced with particles and fibers. In addition, synthetic and natural particles and fibers have been used to enhance durability, thermal properties and shrinkage ratio of lighter geopolymer composites. Owing to the unavailability of a standard for processing and testing geopolymer composites, different laboratories use differing procedures, making data comparison very difficult. The promising market of geopolymer composites for the sustainable construction industry would benefit from a uniform standard for laboratory processing and testing. This would contribute to the creation of a large and reliable data bank, and facilitate the manufacture and certification of geopolymeric sustainable construction materials.

Keywords: Geopolymer, metakaolin, particle composite, fiber composite, kaolin

I. Introduction

Geopolymers (GPs) can be used as a binding phase, replacing ordinary Portland cement (OPC), or to improve the mechanical properties of commercial cements and concretes.

Basic geopolymer processing involves high-shear mixing, molding and curing, similar to the production process of concrete. The optimum curing temperature is between 40–65 °C^{1–4}. Their mechanical properties are superior to OPC in general, but are influenced by the content of liquid phase in the mixture, the curing temperature and the final porosity. They exhibit high fire resistance, withstanding temperatures of 1000–1200 °C^{5–7}. They have high chemical stability, which gives them excellent durability. Compared to OPC concrete mixes, geopolymer cement concrete (GPC) requires much less energy during production, reducing the CO₂ emissions by between 40 % and 80–90 %^{7–13}. Studies indicate that GPCs acquire about 70 % of their final compressive strength in four hours. Full curing occurs by around 28 days, which may result in a GP compressive strength of 100 MPa¹³. Duxson *et al.*^{1, 14–15} carried out extensive research on the relationships between composition, processing, microstructure and the properties of metakaolin-based geopolymers.

Metakaolin (MK) is used as a supplementary cementitious material for OPC. It improves the durability of the resultant binder by reacting with calcium hydroxide

to form hydrated calcium aluminates and silicon aluminates¹⁶. The main constituents of metakaolin are silica and aluminum oxides, with variable contents of other oxides that can be considered as impurities (e.g. Fe₂O₃, TiO₂, CaO, MgO, Na₂O, K₂O).

II. Materials and Methods

(1) Metakaolin GP matrix

Since 2000, researchers have used MK (calcined kaolinite) from different parts of the world to synthesize GPs. Among these, we can enumerate MK from: BASF Germany^{17–24}, France^{25–26}, UK¹, Ukraine²⁷, Australia^{28–30}, China^{31–35}, Czech Republic³⁶, Colombia³⁷, Malaysia³⁸, Brazil^{39–40}, Iran⁴¹, Cameroon³⁵. Table 1 lists the chemical composition and the physical characteristics of these worldwide MKs. The main components are silica (SiO₂, 44.4 %–73 %) and alumina (Al₂O₃, 14.5 %–47.43 %). The MK average particle size (PS) and specific surface area (SSA) ranged from 1.20–38 µm and from 2.16–22 m²/g, respectively (Table 2).

Potassium and/or sodium silicate solution (or water glass) was mostly made by mixing fumed silica with potassium and/or sodium hydroxide pellets dissolved in deionized water and resulting in a myriad of laboratory compositions of the type:



* Corresponding author: ruy@desari.com.br

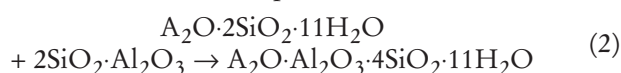
Table 1: Chemical composition (wt%) of MK from different origins.

MK Id.	SiO ₂	Al ₂ O ₃	Fe ₂ O ₃	TiO ₂	CaO	MgO	Na ₂ O	K ₂ O	MnO	SO ₃	P ₂ O ₅	SrO	BaO	CuO	ZrO ₂	PbO	ZnO	Tm ₂ O ₃	LOI ^a
MKA76 Brazil [39]	67.80	29.60	0.70	0.98	0.01		0.01	0.24											0.02
Metamax BASF Germany [20,22]	53.00	43.80	0.43	1.70	0.02	0.03	0.23	0.19		[2 SiO ₂ · Al ₂ O ₃]									
MK-ZK ₂ Iran [41]	73.00	14.50	0.70	0.04	5.00	0.25	0.20	0.20											7.00
Metastar402 UK [1]										[2.3 SiO ₂ · Al ₂ O ₃]									
MK Malaysia [38]	52.68	42.42	2.01	1.46	0.04	0.12	0.07	0.34	0.08	0.05	0.40	0.03							
MK AGS France [25]	54.50	39.50																	
MK Australia [28]	55.90	37.20	1.70	2.40	0.11	0.24	0.27	0.18		0.02	0.17	0.03	0.05						0.80
MK KaolexBN Germany [17-18]				2.60						[65% Kaolin, 7% Muscovite, 2.6% TiO ₂ , 10-30% Crystalline SiO ₂]									
MK HydritePXN Germany [17]			0.60	1.40						[98% Kaolin, impurities: 0.6% Fe ₂ O ₃ , 1.4%TiO ₂]									
MK Ukraine [27]	48.17	36.33	0.36	0.62	0.62	0.30													13.63
MK China [31]	51.91	40.40	0.92	0.76	0.11			0.46		0.10	0.16	0.01		0.02	0.03	0.07	0.05		
Metamax BASF Germany [19,21]	53.00	43.80	0.43	1.70	0.02	0.03	0.23	0.19											0.46
MK Argeco France [26]										[50% MK, 45% Quartz, 1% Calcite, 1% Anatase, 1% Kaolinite, 2% Mullite]									
MK NE Brazil [40]	44.40	39.80	0.30	0.11		0.01	0.04	0.33											14.4
MK Australia [44]										[SiO ₂ /Al ₂ O ₃ =2.01; 1 wt% TiO ₂ , quartz, hematite]									
MK China [30]																			
MK Cameroon [35][1]	54.60	40.60	0.53	0.57	0.12	0.22	0.12	0.53		0.01									2.26
[5 K/min]	52.50	39.04	0.51	0.55	0.11	0.21	0.11	0.51		0.01									6.92
[10 K/min]	52.10	38.74	0.51	0.54	0.11	0.21	0.11	0.51		0.01									6.93
MefistoK05 Czech Rep [36]	55.01	40.94	0.55	0.55	0.14	0.34	0.09	0.6											1.54
MK Australia [29]	54.20	42.10	1.29	1.15	0.13	0.19	0.14	0.20							0.04				0.84
MK BASF Colombia [37]	51.52	44.53	0.48	1.71	0.02	0.19	0.29	0.16											1.09
MK China [33]	51.35	44.24	0.98	0.90	0.13	0.48	0.16	0.08	0.01		0.45								0.72
MK China [34]	45.55	47.43	1.24	2.78								0.44		1.78				0.78	
MK China [32]	55.87	42.25	0.38	0.20	0.04	0.04	0.26	0.31											0.61

^a LOI: loss on ignitionwhere, M_a = alkali mol., A = alkali type (K or Na), M_w = water mol., M_s = silicate mol., M_{wa} = water added mol.

Table 2 lists the various water glass (WG) and GP formulations, and respective WG/MK ratios used by several researchers 1, 17–29, 31–34, 36, 37–39, 41. The MK thermal history ranged from 650 °C up to 900 °C. The WG/MK ratio ranged from 1.38 to 1.86.

Geopolymer was prepared by mixing alkali-water glass and metakaolin in a mixer for 3–30 minutes at 600–1800 rpm to obtain good mixing of the components. In one standard method developed at the University of Illinois at Urbana-Champaign, this slurry was then put by some researchers 17–24, 39 into a planetary conditioning mixer where it was further mixed and degassed for removal of fine bubbles. The GP Si/Al ratio ranged from 1.4 to 8.0 1, 17–29, 31–34, 36, 37–39, 41. The geopolymerization reaction for 2 moles of silicon dioxide and 11 moles of water can be summed up as follows:



This composition was based on TEM/EDS measurements of the “pure” nanoparticulate, nanoporous geopolymer microstructure¹⁷. It corresponded to the

stoichiometric $K_2O \cdot Al_2O_3 \cdot 4SiO_2$ composition of leucite formed when potassium-based geopolymer crystallized upon heating to above 1000 °C in air. The crystallization mechanism was studied *in situ* with high-temperature synchrotron diffraction^{42–43}.

The geopolymer composite slurry was poured into a standard mold attached to a vibration table for more uniform distribution and less void formation. The filled mold was wrapped in plastic film to prevent water loss during setting and curing. Three routes for curing of geopolymers were investigated: pressureless curing, warm pressing, and curing in a high-pressure autoclave¹⁷. Curing time and temperature ranged from 2–24 h at 20–80 °C in a laboratory. Then, the geopolymer composite was demolded and set to dry in a sealed vessel at room temperature. At the required drying age, the samples were tested.

Latella *et al.*⁴⁴ synthesised GPs based on the key precursors NaOH, fumed silica and MK (FSGP), and sodium silicate and MK (SGP) and kept the sealed molds at room temperature for 2 h before curing at 60 °C for 24 h. After the seals had been removed, the samples (25-mm diameter and 40-mm high-compressive cylinders, and flexure bars 6 × 10 × 50 mm) were left at ambient temperature for 4 days before demolding. Mechanical properties were tested (five samples at a cross-head speed of 5 μm/s for compression and 3pt-flexure with support length of 40 mm) after 10 days.

Table 2: Material characteristics and syntheses of MK-based GPs.

MK Id.	GP Si:Al	PS d ₅₀	SSA	MK Thermal Hist.		GP wt%					WG/MK	Mix Speed	Mix Time	Cure Temp	Cure Time
		(μm)	(m ² /g)	(°C)	(h)	Na ₂ O	K ₂ O	Al ₂ O ₃	SiO ₂	H ₂ O		(rpm)	(min)	(°C)	(h)
MKA67 Brazil [71]	4.00	4.74	8.40	700	1.0	2.1	9.6	20.7	40.7	26.9	1.22	933	6	50	24.0
MKM USA [71]	4.00	1.30	13.00			2.5	11.3	16.3	38.4	31.6	1.82	933	6	50	24.0
MKA76 Brazil [71]	4.00	4.74	8.40	700	1.0	9.2		19.9	41.4	29.5	1.30	2500	14	50	24.0
Metamax BASF Germ [72]	4.00	1.30	13.00				14.8	16.1	37.9	31.2	1.86	2000	5	50	24.0
MKA76 Brazil [39]	4.00	4.74	8.40	700	1.0	2.2	10.1	19.3	39.9	28.5	1.38	1800	5	50	24.0
Metamax BASF Germ [22]	4.00	1.30	13.00				14.8	16.1	37.9	31.2	1.86	1600	5	50	24.0
Metamax BASF Germ [20]	3.75	1.20	13.00			11.2		16.8	37.0	35.0	1.71	600	5	70	24.0
MK-ZK ₂ Iran [41]	3.20			700	12.0	10.3		21.3	40.1	28.3		1100	10	20	24.0
Metastar402 UK [1]	3.45	1.58	12.70			10.9		17.9	36.4	34.8			15	40	20.0
	3.70	1.58	12.70			10.6		17.4	38.0	33.9			15	40	20.0
	3.95	1.58	12.70			10.3		17.0	39.6	33.1			15	40	20.0
	4.20	1.58	12.70			10.1		16.6	41.1	32.3			15	40	20.0
	4.45	1.58	12.70			9.8		16.2	42.5	31.5			15	40	20.0
MK Malaysia [38]	3.74	4.25	2.16			13.1		21.5	47.4	18.0		800	5	65	24.0
MK AGS France [25]	3.33	18.60	16.00			9.3		18.5	36.0	36.1				20	24.0
	3.33	18.60	16.00			9.3		18.5	36.0	36.1				60	2.0
	3.33	18.60	16.00			9.3		18.5	36.0	36.1				60	4.0
	3.33	18.60	16.00			9.3		18.5	36.0	36.1				75	2.0
	3.33	18.60	16.00			9.3		18.5	36.0	36.1				75	4.0
MK Australia [28]															
[1.4-650-20]	2.90	38.00		650	1.0	9.7		24.2	41.3	24.8			5	20	24.0
[1.4-700-20]	2.90	38.00		700	1.0	9.7		24.2	41.3	24.8			5	20	24.0
[1.4-750-80]	2.90	38.00		750	1.0	9.7		24.2	41.3	24.8			5	80	24.0
[1.4-750-20]	2.90	38.00		750	1.0	9.7		24.2	41.3	24.8			5	20	24.0
[1.4-800-20]	2.90	38.00		800	1.0	9.7		24.2	41.3	24.8			5	20	24.0
[1.54-650-20]	3.04	38.00		650	1.0	5.5		21.6	38.6	34.3			5	20	24.0
[1.54-700-20]	3.04	38.00		700	1.0	5.5		21.6	38.6	34.3			5	20	24.0
[1.54-750-20]	3.04	38.00		750	1.0	5.5		21.6	38.6	34.3			5	20	24.0
[1.54-750-80]	3.04	38.00		750	1.0	5.5		21.6	38.6	34.3			5	80	24.0
[1.54-800-20]	3.04	38.00		800	1.0	5.5		21.6	38.6	34.3			5	20	24.0
MK KaoIexBN Germany [17]	4.00		22.00	700	1.0		12.5	20.8	40.4	26.3				45	24.0
MK KaoIexBN German [18]	4.00		22.00	700	1.0		12.5	20.8	40.4	26.3				45	24.0
MK HydritePXN Germ [17]	4.00	1.70	18.01	700	10.0		14.7	16.3	38.0	31.0				45	24.0
MK Ukraine [27]	4.00					10.6		17.4	41.1	30.8				80	6.0
	6.00					7.8		12.8	45.4	34.0				80	6.0
	8.00					6.2		10.1	47.8	35.9				80	6.0
MK China [31]	4.00	4.08		800	2.0		14.8	16.1	37.9	31.2		1600	30	120	24.0
Metamax BASF Germ[21]Na	4.00	1.30				10.3		16.9	39.9	32.9		1800	5	50	24.0
K	4.00	1.30					14.8	16.1	37.9	31.2		1800	5	50	24.0
Metamax BASF Germany															
[19]															
K1.5-24	3.00	1.30					16.4	17.7	31.4	34.5		vacuum	23	80	24.0
K1.5-48	3.00	1.30					16.4	17.7	31.4	34.5		vacuum	23	80	48.0
K2-24	4.00	1.30					14.8	16.1	37.9	31.2		vacuum	23	80	24.0
K2-48	4.00	1.30					14.8	16.1	37.9	31.2		vacuum	23	80	48.0
Na1.5-24	3.00	1.30				11.4		18.8	33.2	36.5		vacuum	3	80	24.0
Na1.5-48	3.00	1.30				11.4		18.8	33.2	36.5		vacuum	3	80	48.0
Na2-24	4.00	1.30				10.3		16.9	39.9	32.9		vacuum	3	80	24.0
Na2-48	4.00	1.30				10.3		16.9	39.9	32.9		vacuum	3	80	48.0
MK Argeco France [26]	3.60					9.2		16.8	35.6	38.5			95% RH	20	168.0
MK NE Brazil [40]	4.30	4.24				12.5		16.5	41.8	29.2				65	2.5
MK Australia [44]	FSGP	3.00		750	15.0	7.5		24.7	43.7	24.0			amb 2h	60	24.0
SGP	3.00			750	15.0	13.1		21.5	38.0	27.4			amb 2h	60	24.0
MK China [30]	5.50			700	12.0	10.0		16.4	53.3	20.3		slow	3	20	24.0
MK Cameroon [35][1K/min]	5.30	14.00	12.87	700	0.5	9.8		16.2	50.5	23.4			98% RH	20	24.0
[5K/min]	5.30	14.00	12.95	700	0.5	9.8		16.2	50.5	23.4			98% RH	20	24.0
[10K/min]	5.30	14.00	12.55	700	0.5	9.8		16.2	50.5	23.4			98% RH	20	24.0
Mefisto Czech Rep [36]20C	3.26	4.82	13.10	750		11.3		18.6	35.8	34.2			5	20	4.0
40C	3.26	4.82	13.10	750		11.3		18.6	35.8	34.2			5	40	4.0
60C	3.26	4.82	13.10	750		11.3		18.6	35.8	34.2			5	60	4.0
80C	3.26	4.82	13.10	750		11.3		18.6	35.8	34.2			5	80	4.0
MK Australia [29]	4.50			750	24.0	12.4		15.7	41.5	30.4				75	24.0
MK BASF Colombia [37]	4.50	7.80					11.3	17.5	46.4	24.7				70	20.0
MK China [33]	4.40	17.00		900	6.0		11.5	12.5	32.3	43.7			12	20	168.0
MK China [34]	4.00					16.1		15.8	37.3	30.8				20	24.0
MK China [32]	20C	3.20	8.00	12.00	750	2.0	9.8	16.2	30.5	43.5				20	24.0
80C-SC	3.20	8.00	12.00	750	2.0	9.8		16.2	30.5	43.5				80	24.0
80C-WC	3.20	8.00	12.00	750	2.0	9.8		16.2	30.5	43.5				80	24.0

Yunsheng *et al.*³⁰ used China kaolin calcined at 700 °C for 12 h. NaOH and sodium silicate solution having a molar ratio of $\text{SiO}_2/\text{Na}_2\text{O}$ of 3.2 and a solid content of 37 % were used. NaOH, sodium silicate solution and water were mixed in a beaker and cooled down to room temperature. Then, calcined kaolin and silica were slowly added and mixed for 3 min. Fresh slurry was poured into six cubic steel molds measuring 40 mm by 40 mm by 40 mm for each formulation. Samples were vibrated for 2 min on the vibration table. The specimens were covered with plastic films during setting and the mold was removed after 24 h. The demolded specimens were cured at 20 °C and 95 % RH for 28 days.

Kenne *et al.*³⁵ used Cameroon kaolin maintained at ambient laboratory temperature for a week, cured at 105 °C until its mass became constant and then it was ground and sifted through a sieve of mesh 90 μm . Then, the dried kaolin was calcined at 700 °C for 30 min with varying rate of calcination (1, 2.5, 5, 10, 15 and 20 K/min) to obtain MKs, which were used to produce geopolymers. The alkaline solution was prepared by mixing sodium silicate and sodium hydroxide solution (12 M) to obtain a $\text{Na}_2\text{O}/\text{SiO}_2$ molar ratio of 0.7. Sodium silicate was made up of SiO_2 (26.5 wt%), Na_2O (8.0 wt%) and H_2O (65.5 wt%). GP paste was prepared by mixing alkaline solution with MK powder according to a liquid/solid mass ratio of 1:1 in an automatic Hobart mixer. Compressive strength cubic samples of (20 × 20 × 20 mm) were made by mixing standardized sand and MK powder and alkaline solution in mass ratio of 3:1:1. Specimens were cured at 20 °C in a controlled room at 20 ± 2 °C and 98 % RH. The specimens were demolded 24 h later and the cubic samples were covered with polyethylene film and stored at ambient temperature (20 °C) under 98 % RH condition for 28 days.

Kenne *et al.*³⁵ applied a compressive strength loading rate of 0.2 kN/s. Hardened geopolymer pastes aged 28 days were crushed and sifted through a sieve of mesh 80 μm and the powder was subjected to XRD. Bulk density and specific surface area of MKs (1, 2.5, 5, 10, 15, 20 K/min) ranged from 2.54–2.56 g/cm³ and 12.549–12.979 m²/g, respectively. The average particle size (d_{50}) was 14 μm and the chemical composition (mass%) of K was as follows: SiO_2 (47.2), Al_2O_3 (35.1), Na_2O (<0.1), K_2O (0.46), Fe_2O_3 (0.46), TiO_2 (0.49), CaO (<0.1), SO_3 (<0.01) and loss on ignition (14.94). Thermal analysis of the clay fraction first event went up to 100 °C and corresponded to elimination of water of hydration. The second event lay between 225 and 300 °C with mass loss of 2.09 % and corresponded to the dehydroxylation of gibbsite. The third event between 450 and 550 °C with mass loss of 9.49 % represented the dehydroxylation of kaolinite and gave rise to a mass percentage of kaolinite to 81 %.

Rovnaník³⁶ analyzed the effect of curing temperature (10, 20, 40, 60 and 80 °C) and time on the compressive and flexural strengths, pore distribution and microstructure of Mefisto K05 Czech Republic metakaolin-based geopolymer. MK was produced by means of calcination of kaolin at 750 °C in a rotary kiln. The molar composition of MK was as follows: SiO_2 (55.01), Al_2O_3 (40.94), Na_2O (0.09), K_2O (0.60), Fe_2O_3 (0.55), TiO_2 (0.55), CaO (0.14), MgO

(0.34), LOI (1.54). The surface area was 13.1 m²/kg, and the mean particle size (d_{50}) was 4.82 μm . Alkaline silicate solution having a silicate modulus ($\text{SiO}_2/\text{Na}_2\text{O}$) of 1.39 was prepared by dissolving solid sodium hydroxide (98.0 %) in commercial sodium water glass ($\text{SiO}_2/\text{Na}_2\text{O} = 3.26$ and $\text{H}_2\text{O}/\text{Na}_2\text{O} = 10.40$). Quartz sand with a maximum grain size of 2.5 mm was added as an aggregate. Geopolymer samples were prepared by mechanically mixing MK and activator solution in a planetary mixer for 5 min. Then quartz sand was mixed into this geopolymer paste with some additional water. The slurry was cast into prismatic molds with dimensions 40 × 40 × 160 mm, vibrated for 2 min to remove entrained air and sealed. In the first experiment, the specimens were cured at temperatures from 10 to 80 °C. One set of specimens was stored at an ambient temperature (20 °C) and considered a reference material, one was stored in a refrigerator (10 °C) for the whole period before testing, and other specimens were cured at temperature 40, 60 or 80 °C in an electrical oven immediately after casting. After 4 h they were removed from the oven and stored at an ambient temperature (20 °C) and relative humidity 45 ± 5 % until tested. The second experiment was focused on the effect of different curing times at elevated temperatures. The specimens were treated for 1, 2, 3 and 4 h at temperatures of 40, 60 or 80 °C.

Rowles and O'Connor²⁹ prepared GPs with Si:Al and Na:Al molar ratios, ranging between 1.08–3.0 and 0.51–2.0, respectively. The starting materials were: a crystalline Australian kaolinite, an amorphous silica fume (SF), and analytical-reagent-grade sodium hydroxide pellets. MK was obtained by heating the kaolinite at 750 °C in air for 24 h. MK was verified to be amorphous by means of XRD, except for quartz and anatase impurities. The chemical compositions of the MK and SF materials were, respectively: SiO_2 (54.2, 94.2), Al_2O_3 (42.1, 0.15), Fe_2O_3 (1.29, 0.49), MgO (0.19, 0.05), CaO (0.13, <0.01), Na_2O (0.14, 0.04), K_2O (0.20, 0.01), TiO_2 (1.15, 0.03), ZrO_2 (0.04, 3.69), LOI (0.84, 0.86), Total (100.28, 99.52). The samples were cast in closed molds and heated to 75 °C for 24 h. After the curing period, the samples were kept in their molds for 7 days in ambient conditions before being removed for microstructural characterization.

Rowles and O'Connor²⁹ carried out SEM microscopy using a Philips XL30. Elemental analyses were carried out using an Oxford Instruments energy-dispersive spectrometer (EDS). Samples were prepared by mounting the polymer in epoxy resin and polishing to 1 μm . Samples were cleaned by means of sonication after each step in the polishing process to remove excess polishing media and debris. The polished samples were dried overnight in an oven at 40 °C. The drying process introduced shrinkage cracks for some samples owing to the samples' original moisture content and their uptake of polishing media. The measurement conditions of the SEM (accelerating voltage 20 kV, beam current 60 pA, working distance 10.4 mm, spectrum collection time 100 s) were standardized to allow for maximum repeatability in experimental conditions between sample batches. Secondary electron imaging was used for imaging, with back-scattered electron imaging being used to identify high atomic num-

ber impurities. For each sample, five regions of interest of $300\text{ }\mu\text{m} \times 200\text{ }\mu\text{m}$ were investigated. On each of these regions, EDS spectra were collected over the entire area, for five points on grains and for five points within the matrix. To limit bias introduced by the interaction volume, the locations of the spot analyses were chosen such that there were no other phases visible on the surface within $5\text{ }\mu\text{m}$. Quantitative analysis of the inorganic polymer elemental composition was carried out using internal software calibration and referenced against standard kaolinite and MK.

The precursor materials selected by Villaquirán-Cacedo and Gutiérrez³⁷ were: BASF MK, rice husk ash (RHA), and KOH. The chemical compositions of the MK and RHA materials were, respectively: SiO_2 (51.52, 92.33), Al_2O_3 (44.53, 0.18), Fe_2O_3 (0.48, 0.17), MgO (0.19, 0.49), CaO (0.02, 0.63), Na_2O (0.29, 0.07), K_2O (0.16, 0.15), TiO_2 (1.71, 0.0), LOI (1.09, 2.57). The MK particle size was $7.8\text{ }\mu\text{m}$. RHA was used as the silica source to prepare the activator. The RHA was obtained via thermal treatment of the rice husk at $700\text{ }^\circ\text{C}$ for 2 h in an electric oven; the amorphous SiO_2 content in the RHA was 92 %. The alkaline solution used as the activating agent was prepared from the RHA mixture with potassium hydroxide pellets in the presence of water. In the mixture, a $\text{SiO}_2/\text{Al}_2\text{O}_3$ molar ratio of 2.5 and a liquid/solid molar ratio of 0.4 were used; the $\text{K}_2\text{O}/\text{SiO}_2$ molar ratio was 0.28. The specimens were cured at a temperature of $70\text{ }^\circ\text{C}$ for 20 h at a relative humidity $> 90\text{ }\%$. Afterwards, they were demolded, wrapped in plastic film to avoid water evaporation, and placed in a chamber at a relative humidity of $\sim 60\text{ }\%$. Then, the compressive strengths at different curing ages were determined.

The GP precursor powder used by Zhang *et al.*³³ was China K calcined under $900\text{ }^\circ\text{C}$, with an average particle size of $17\text{ }\mu\text{m}$. The chemical composition of MK was: SiO_2 (51.35), Al_2O_3 (44.24), Fe_2O_3 (0.98), MgO (0.48), CaO (0.13), Na_2O (0.16), K_2O (0.08), TiO_2 (0.90), P_2O_5 (0.45), MnO (0.01), LOI (0.72). The alkaline activator solution was formulated by blending commercial potassium silicate solution, potassium hydroxide flakes with 90 % purity, and tap water to obtain the desired $\text{SiO}_2/\text{K}_2\text{O}$ molar ratio of 1.0. The chemical composition of commercial potassium silicate solution was $\text{K}_2\text{O} = 15.8\text{ wt}\%$, $\text{SiO}_2 = 24.2\text{ wt}\%$, and $\text{H}_2\text{O} = 60\text{ wt}\%$, and $\text{SiO}_2/\text{K}_2\text{O}$ molar ratio equaled 2.4. Activator solutions were prepared 1 day prior to use. The solid-to-liquid ratio, representing mass ratio of aluminosilicate precursor to alkaline activator solution, was adopted as 0.8. The water content (ratio of the mass of solvent in the activator solution to the total mass of precursor and solution) was 31 %.

Zhao *et al.*³⁴ used commercial China MK as an aluminosilicate source for synthesis of geopolymeric matrix. The chemical composition of MK included 47.43 wt% Al_2O_3 , 45.55 wt% SiO_2 , 2.78 wt% TiO_2 , 1.78 wt% CuO , 1.24 wt% Fe_2O_3 , 0.44 wt% SrO , and 0.78 wt% Tm_2O_3 . The sodium silicate containing 79.17 wt% SiO_2 , 19.79 wt% Na_2O and 1.04 wt% Al_2O_3 was commercially supplied, together with sodium hydroxide (NaOH).

The geopolymer binder used by Zhu *et al.*³² was synthesized by activation of metakaolin with sodium sil-

icate solution. The metakaolin was obtained from Fujian province, China. It was a product of kaolin powder heated to $750\text{ }^\circ\text{C}$ for 2 h. The metakaolin powder had a BET surface area of $12\text{ m}^2/\text{g}$, and the average particle size of $8\text{ }\mu\text{m}$. The chemical composition of MK was: SiO_2 (55.87), Al_2O_3 (42.25), Fe_2O_3 (0.38), MgO (0.04), CaO (0.04), Na_2O (0.26), K_2O (0.31), TiO_2 (0.20), LOI (0.61). The alkaline activator was a mixture of chemical grade NaOH solution (12 M) and commercial liquid sodium silicate (original modulus was 3.33, Na_2O 8.29 wt%, SiO_2 29.91 wt%). The mass ratio of NaOH solution and the liquid sodium silicate was 0.7, giving a molar ratio $\text{SiO}_2:\text{Na}_2\text{O}$ of 1.2 in the mixture. Distilled water was then added to adjust the concentration to 35 wt% ($\text{Na}_2\text{O} + \text{SiO}_2$) and the molar ratio of $\text{H}_2\text{O}/\text{Na}_2\text{O}$ was 15.2.

(2) Particles and fibers

Particle and fiber reinforcements have been used to increase the flexure strength and toughness of MK-based geopolymer materials. Synthetic particles and fibers, such as steel¹⁸, aluminum²⁰, polypropylene²⁰, carbon nanotubes²⁰, slag⁴⁵, polyacetal³⁴ have been investigated. In addition, natural particles and fibers, such as basalt^{17–18, 21–22, 45–46}, palm oil fuel ash³⁸, corn husk⁴⁷, wool⁴⁸, jute⁴⁹, rice stem⁵⁰, fique⁵¹, malva⁵² and bamboo^{23–24, 39, 53}, have been investigated.

Zhao *et al.*³⁴ studied MK-based GP reinforced with polyacetal (POM) fibers; China resins of low-viscosity acetal copolymer, with a high modulus of 6.96 GPa, high tensile strength of 925 MPa, and moderate elongation of 15.6 %. The fiber bundle was cut into short fibers having lengths of 3, 6, and 9 mm. The metakaolin-based geopolymers could usually be synthesized based on the reaction of metakaolin powders, sodium silicate, and an alkaline solution containing NaOH at room temperature. In a typical synthetic process, an alkaline activator was first prepared by mixing an aqueous solution of sodium silicate with NaOH, in which the molar ratio of $\text{SiO}_2/\text{Na}_2\text{O}$ was adjusted to 1.2:1. Then, the geopolymer paste was prepared by mixing the metakaolin powders with the alkaline activator at a Si/Al molar ratio of 2:1. In succession, the short POM fibers were added into the geopolymer paste under vigorous agitation to prepare a series of pre-curing pastes having different fiber contents and lengths. These pre-curing geopolymer pastes were fed into the stainless molds with different cavity dimensions and then cured at room temperature for 24 h. The geopolymeric specimens with different dimensions were formed for further mechanical and tribological measurements.

(3) Geopolymer composites (GPC) testing

Villaquirán-Cacedo and Gutiérrez³⁷ reported that the compressive strength was determined for each of the geopolymeric systems up to an age of 180 curing days using cubic specimens with dimensions of $20 \times 20\text{ mm}$; the test was performed at a displacement rate of $1\text{ mm}/\text{min}$.

Sá Ribeiro *et al.*^{24, 39, 53} and Sankar *et al.*²³ bamboo-reinforced geopolymer composite samples were subjected to third-point loading flexural strength testing, according to ASTM standard C1341–13²⁵. The average density of bamboo-reinforced geopolymer composites was

1.35 g/cm³. The test span-to-depth ratio was 25:1, and the crosshead displacement rate was 0.10 mm/s. Strain was measured based on crosshead displacement.

Yunsheng *et al.*³⁰ performed compressive tests according to ASTM C39–96. The loading was displacement-controlled at a constant rate of 1.3 mm/min. The GP optimum formulation was Na₂Si₆Al₂O₁₆·2H₂O with SiO₂/Al₂O₃ = 5.5, Na₂O/Al₂O₃ = 1.0 and H₂O/Na₂O = 7.0.

Rovnaník³⁶ conducted mechanical tests on specimens made of geopolymers mortars with quartz sand at the age of 1, 3, 7 and 28 days. Flexural strengths were determined using standard three-point-bending test, and compressive strengths were measured on the far edge of both residual pieces obtained from the flexural test according to the EN 196–1 standard.

Zhang *et al.*³³ prepared GP pastes by pouring alkaline silicate solution into aluminosilicate source material (MK powder), and then mixing them in a mixer for 12 min. To obtain specimens for bending and compression tests, geopolymer pastes were cast into steel molds of size 160 × 40 × 40 mm and then vibrated on a shake table to remove any air bubbles. After they had been covered with plastic films, the specimens were cured at a constant temperature of 20 °C and a humidity of 90 % for 7 days. The bending tests on geopolymer composites at ambient temperature were conducted according to ASTM C348. The central distance between two supporting ends of the specimen was adjusted to be 100 mm. The load was applied at the mid-span of the specimen, and increased at a rate of 50 N/s until the specimen broke into two parts. Then the compression test was carried out on the two broken parts separately. The compression area of the test specimen was 40 × 40 mm, and the loading velocity was kept at 2 500 N/s.

Zhao *et al.*³⁴ measured the flexural strength of geopolymeric composites in a universal testing machine using a three-point bending fixture with a load cell of 110 kN at a crosshead speed of 0.5 mm/min according to ISO 679–2009 standard. The compressive strength of geopolymeric composites was also determined using the universal testing machine at a compressive rate of 5 mm/min according to ISO 679–2009 standard. All the measurements were carried out at room temperature, and each of the reported mechanical data represented an average value of five tests.

Zhu *et al.*³² cast compression testing geopolymer paste into cubic specimens of size 20 × 20 × 20 mm and allowed these to harden at 20 °C air curing at a relative humidity of 95 ± 5 % conditions. The 1-day-aged geopolymer specimens were put in the following conditions for further curing until testing: (1) AC – 20 °C air curing at relative humidity of 95 ± 5 %; (2) SC – 80 °C sealed curing in plastic bags; and (3) WC – 80 °C water curing in a water bath. Compressive strength testing was performed in a universal mechanical testing machine, at a load rate of 0.5 mm/min. The compression-fractured specimens at different ages were collected and stored in acetone. The samples were ground and dried at 65 °C for 24 h for XRD.

III. Results and Discussion

With basalt fiber reinforcement, the bending strength of the GPC increased from 2.8 MPa to 10.3 MPa^{17–18}. The addition of 10 wt% of basalt fibers measuring 13 μm in diameter × 6.35 mm in length to potassium-based geopolymer composites yielded 19.5 MPa three-point flexure strength⁴⁵. Increasing the chopped basalt fiber length to 12.7 mm yielded 27.07 MPa three-point flexure strength⁴⁶. Sodium-based geopolymer reinforced with corn husk fiber bundles resulted in 14.14 MPa four-point flexure strength⁴⁷. Sodium-based geopolymer reinforced with 5 wt% wool fiber bundles yielded 8.1–9.1 MPa three-point flexure strength⁴⁸. Sodium-based geopolymer reinforced with 30 wt% untreated jute weave resulted in 20.5 MPa four-point flexure strength⁴⁹. Potassium-based geopolymer reinforced with 6.4 wt% rice stem yielded 18.45 MPa three-point flexure strength⁵⁰. Potassium-based geopolymer reinforced with 30 wt% alkali-treated fique fibers yielded 11.4 MPa four-point flexure strength⁵¹. Sodium-based geopolymer reinforced with 5.5 wt% of unidirectional untreated malva resulted in 31.5 MPa four-point flexure strength⁵². Recent works on metakaolin-based geopolymer reinforced with bamboo fibers (BFs) revealed 30 MPa and 7 MPa average compressive and flexural strengths, respectively, of GP with 5 wt% (8 vol%) BF³⁹. In addition, average flexural strength of 25 MPa for the mixed bamboo fiber-strip-reinforced GPC were recorded³⁹. Additional research results are summarized in Tables 3–5.

Pouhet *et al.*²⁶ reported the ability of flash-calcined metakaolin and sodium silicate to completely substitute known hydraulic binders, in terms of workability and compressive strength. She also reported durability issues in alkali-silica reaction and carbonation. Alkali-silica reaction would not be detrimental in a matrix of metakaolin activated by sodium silicate. Very rapid reaction of the alkalis in the geopolymer paste pore solution with atmospheric CO₂ did not lead to a significant drop of the concrete pH. A study was also conducted on the influence of the water glass solution used on the mechanical performance of geopolymer. The higher the sodium concentration of the initial activation solution, the smaller the standard deviation of the measured values. Addition of sodium hydroxide for the preparation of the activation solution led to greater dispersions of the strength values. Solution Wg1.7 was chosen. Using an Na-GP formulation of 0.9 Na₂O·Al₂O₃·3.6 SiO₂·13 H₂O, resulted in 7-day-average compressive and 3pt-flexure strength values of 62 MPa and 8.5 MPa, respectively, from samples cured at 20 °C and 95 % RH.

The investigations reinforcing Amazonian geopolymer composite with bamboo fibers and strips resulted in the following observations by Sá Ribeiro *et al.*^{24,39,53}: (1) XRF chemical analysis of Amazonian kaolinite (KA) and metakaolinite (MKA) confirmed the major components to be alumina and silica. (2) SEM micrographs of the structure of the 75 %-K, 25 %-Na MKA-based (K75Na25-MKA76) GP revealed some unreacted MK and the presence of crystalline quartz. SEM and digital images of the mixed alkali-MKA-bamboo fiber (K75Na25-MKA76-

Table 3: Physical and compressive strength properties of MK-based GPCs.

MK Id.	GP Type	Density		Compressive Strength								
		(g/cm ³)	Ø (mm)	d (mm)	b (mm)	Samples	r (mm/s)	1d (MPa)	3d (MPa)	7d (MPa)	14d (MPa)	28d (MPa)
MKA67 Brazil [71]	K75-Na25	1.81	5.00	12.0		9	0.0001			58.0		
MKM USA [71]	K75-Na25	1.77	5.00	12.0		9	0.0001			70.5		
MKA76 Brazil [71]	Na	1.70	5.00	12.0		9	0.0001			83.5		
Metamax BASF Germ [72]	K		3.00	6.0		20	0.0083			101.0		
MKA76 Brazil [39]	K75-Na25	1.75	25.00	50.0		6	0.0100			55.7		
Metamax BASF Germ [20]	Na	1.61	50.00	100.0		3	.25MPa/s			54.0		
MK-ZK ₇ Iran [41]	Na			50.0	50.0	5				13.9	29.6	42.6
Metastar402 UK [1]	Na1.15	1.68	25.00	50.0		6	0.0100			15.0		
	Na1.40	1.70	25.00	50.0		6	0.0100			37.5		
	Na1.65	1.72	25.00	50.0		6	0.0100			57.5		
	Na1.90	1.78	25.00	50.0		6	0.0100			76.3		
	Na2.15	1.80	25.00	50.0		6	0.0100			63.8		
MK Malaysia [38]	Na-20-S35-P45	1.91		50.0	50.0	3			43.2	45.0	46.5	48.0
MK AGS France [25]	Na-20C-24h			40.0	40.0					68.2		
	Na-60C-2h			40.0	40.0					31.3		30.6
	Na-60C-4h			40.0	40.0					30.6		34.3
	Na-75C-2h			40.0	40.0					28.9		29.4
	Na-75C-4h			40.0	40.0					34.0		39.8
MK Australia [28]	1.4-700-20			25.0	25.0		.33MPa/s		23.4			
	1.4-750-20			25.0	25.0				26.2			
	1.54-700-20			25.0	25.0				42.7			
	1.54-750-20			25.0	25.0				45.1			
	1.54-750-80			25.0	25.0				33.5			
	1.46-750-20			25.0	25.0				38.9			
	1.46-750-80			25.0	25.0				20.5			
	1.50-750-20			25.0	25.0				39.3			
	1.50-750-80			25.0	25.0				26.0			
	1.52-750-20			25.0	25.0				44.4			
	1.52-750-80			25.0	25.0				28.0			
	1.80-750-20			25.0	25.0				31.4			
	1.80-750-80			25.0	25.0				30.2			
MK KaolexBN Germ [17]	2.05-750-20			25.0	25.0				22.1			
	2.05-750-80			25.0	25.0				20.8			
	K		6.25	25.0		14				59.0		
	K		6.25	25.0		14				59.0		
	K		6.25	25.0		13				37.0		
	Na4			20.0	20.0					26.0		
	Na6			20.0	20.0					40.0		
	Na8			20.0	20.0					45.0		
	Metamax BASF Germ [21]	1.51	5.00	12.6			100N/min			75.5		
	K	1.47	5.00	12.6			100N/min			109.0		
	Metamax BASF Germ [19]	K-1.5-24	1.46			15	0.0100	32.0				
		K-2-24	1.68			15	0.0100	26.1				
		K-1.5-48	1.46			15	0.0100	33.3				
MK Argeco France [26]		K-2-48	1.68			15	0.0100	30.1				
		Na-1.5-24	1.38			15	0.0100	32.1				
		Na-2-24	1.50			15	0.0100	26.6				
		Na-1.5-48	1.38			15	0.0100	37.1				
		Na-2-48	1.50			15	0.0100	26.4				
	Na	1.34		40.0	40.0	3				62.0		
	Na	1.41						52.0	49.0	48.0	1h	
	MK NE Brazil [40]											
	MK Australia [44]	FSGP	1.42	25.00	40.0	5	0.0050				35.0	
		SGP	1.46	25.00	40.0	5	0.0050				72.0	
	MK China [30]	Na		40.0	40.0	6	0.0217					34.9
	MK Cameroon [35][1]	Na-1C/min		20.0	20.0		200N/min					49.4
		[5K/min]		20.0	20.0		200N/min					36.0
		[10K/min]		20.0	20.0		200N/min					31.0
MefistoK05 Czech Rep [36]	Na-20C	2.09		40.0	40.0			16.0	52.0	58.0		62.0
	40C	2.03		40.0	40.0			37.0	58.0	61.0		62.0
	60C	1.98		40.0	40.0			47.0	46.0	50.0		48.0
	80C	1.96		40.0	40.0			52.0	47.0	51.0		51.0
MK Australia [29]	Si:Na=1.5/1.0									23.4		
	Si:Al/Na:Al=2.0/1.0									51.3		
	Si:Al/Na:Al=2.0/1.29									53.1		
	Si:Al/Na:Al=2.5/1.0									45.0		
	Si:Al/Na:Al=2.5/1.29									64.0		
	Si:Al/Na:Al=2.5/1.53									49.0		
	Si:Al/Na:Al=3.0/1.53									26.0		
	Si:Al/Na:Al=3.0/2.0									19.9		
MK BASF Colombia [37]	K			20.0	20.0		0.0167			41.0		42.0
MK China [33]	K	2.31		40.0	40.0	6	2500 N/s			50.0		
MK China [34]	Na-0					5	0.083	49.0				
MK China [32]	20C-AC			20.0	20.0		0.0083			60.0		67.0
	80C-SC			20.0	20.0		0.0083			69.0		46.0
	80C-WC			20.0	20.0		0.0083			77.0		67.0

Table 4: Physical and four-point flexural strength properties of MK-based GPCs.

MK Id.	GP Type	Density (g/cm ³)	4Pt Flexural Strength								
			L (mm)	d (mm)	b (mm)	Samples	r (mm/s)	1d (MPa)	7d (MPa)	14d (MPa)	28d (MPa)
Metamax BASF Ger [72]	K	1.47	40.0	10.0	10.0		23 N/min		7.5		
Metamax BASF Germ [22]	K	1.47	40.0	1.6	10.0	6	0.001		4.5		
MK-ZK ₂ Iran [41]	Na		150.0	19.0	28.0	5			4.6	4.7	5.3
MK KaolexBN Germ [17]	K		150.0	25.0	25.0	6			2.8		
MK KaolexBN Germ [18]	K		150.0	25.0	25.0	6			2.8		
Metamax BASF Germ [21]	Na	1.51	40.0	10.0	10.0		0.001		14.1		
	K	1.47	40.0	10.0	10.0		0.001		8.7		

Table 5: Physical and three-point flexural strength properties of MK-based GPCs.

MK Id.	GP Type	Density (g/cm ³)	3Pt Flexural Strength									
			L (mm)	d (mm)	b (mm)	Samples	r (mm/s)	1d (MPa)	3d (MPa)	7d (MPa)	14d (MPa)	28d (MPa)
MKA76 Brazil [71]	Na		40	10	10	7	0.010	10.5				
MK China [31]	K		30	4	3	6	0.008			16.8		
MK Argeco France [26]	Na	1.34	160	40	40	3				8.5		
MK Australia [44]	FSGP	1.42	40	6	10	5	0.005				3.1	
	SGP	1.46	40	6	10	5	0.005				10.8	
MefistoK05 Czech Rep [36]	Na-20C	2.09	160	40	40			4.0	10.0	11.5		11.6
	40C Na	2.03	160	40	40			8.0	11.4	11.4		11.4
	60C Na	1.98	160	40	40			10.5	11.3	9.4		10.0
	80C Na	1.96	160	40	40			10.6	9.7	9.9		10.6
MK China [33]	K	2.31	100	40	40	6	50 N/s			5.4		
MK China [34]	Na-0					5	0.008	4.3				

BF4W) GPC tested for 4-pt flexural strength revealed imprints of the pulled-out bamboo fibers and BF pull-out, with no abrupt rupture, denoting force transfer between the bamboo fibers and the geopolymer matrix. (3) The BF-reinforced GP compressive strengths of 25 × 50-mm tested samples were lower (23–38 MPa) than that of pure GP (56 MPa), but still met the requirements for use in sustainable structural applications. (4) There was no difference in 4-point flexural strength between the alkali and water treatment of the bamboo fibers and strips. Adding bamboo strips to the GPC reinforced with bamboo fibers increased the flexural strength by about 3.5 times. The stress-strain curves were smooth, and yielded a reasonable average flexural strength of 7 MPa for the fiber-reinforced GPC, and high average flexural strength of 25 MPa for the mixed fiber-strip-reinforced GPC. (5) Design, fabrication and evaluation of mixed mode compounds containing chopped fibers inter-dispersed between long slices of bamboo revealed the bamboo-reinforced geopolymer composite to be a potential sustainable green material for construction.

Barbosa *et al.*⁴⁰ used an Na-GP formulation of 1.25 Na₂O·Al₂O₃·4.3 SiO₂·10 H₂O, with samples matured at room temperature for 1 h, cured at 65 °C for 1.5 h, and dried at 65 °C for 1 h. The resulting average compressive strength values aged for 1 h, 24 h and 3 days were 48, 52 and 49 MPa, respectively.

Latella *et al.*⁴⁴ reported based on EDS analyses that the lower the Na/Al ratio (0.5 and 0.6 for furnace slag geopolymer (FSGP) and slag geopolymer (SGP), respectively), the less Na is available for binding to form a coherent solid. FSGP and SGP presented density and poros-

ity values of 1.42 g/cm³, 20 %, and 1.46 g/cm³, 25 %, respectively. The highest compressive strength value obtained was for SGP (72 ± 5 MPa). FSGP yielded only 35 ± 5 MPa compressive strength. Three-point MOR and E for SGP and FSGP were 10.8 ± 0.7 MPa, 9.6 ± 0.3 GPa, and 3.1 ± 1.5 MPa, 5.3 ± 0.6 GPa, respectively. SEM images of polished surfaces in the densified regions of the two GPs showed that SGP was denser compared with FSGP. However, it also had some unreacted MK grains scattered throughout the matrix.

Yunsheng *et al.*³⁰ reported that the Na₂O/Al₂O₃ and H₂O/Na₂O had a very important impact on the compressive strength (34.9 MPa), while the SiO₂/Al₂O₃ had little influence. Macroscopic and microscopic results revealed that an almost fully reacted Na-PSDS geopolymer could be obtained at the molar ratio SiO₂/Al₂O₃ = 5.5, Na₂O/Al₂O₃ = 1.0 and H₂O/Na₂O = 7.0. Microscopic analysis showed structural characteristics similar to solidified gels.

Kenne *et al.*³⁵ reported that the rate of calcination of kaolin had no significant effect on the bulk density of metakaolins. The SiO₂/Al₂O₃ molar ratio was 2.28. The XRD halo peak with 2θ between 18° and 38° for metakaolins was now located between 20° and 45° for geopolymers, which is the XRD fingerprint of geopolymerization. The lower the rate of calcination, the more complete was the transformation of kaolin into metakaolin. Residual kaolinite was mainly responsible for the increase of the loss on ignition, which was a good indication of the presence of reactive phase: the higher the loss on ignition, the less reactive phase contained by the metakaolin allowing for geopolymer synthesis. As the

rate of calcination of kaolin increased, the setting time increased (226 min (rate of 1 K/min)-692 min (5°)-693 min (10°)-773 min (rate of 20 K/min)) while the compressive strength was reduced (49.4 MPa (rate of 1 K/min)-36 MPa (5°)-31 MPa (10°)-20.8 MPa (rate of 20 K/min)). Compressive strengths of geopolymers were higher for metakaolin that did not contain residual kaolinite and this was achieved when kaolin was calcinated at a low heating rate. From the results obtained, it was concluded that the production of geopolymers having high compressive strength along with low setting time required that the calcination of kaolin be carried out at a low rate.

Rovnanik³⁶ reported that almost all tested specimens set and formed hard structures within 24 h after preparation, except for the specimens that were cured under low temperature conditions. A temperature of 10 °C retarded the setting and hardening of a geopolymer mixture to 4 days. Reference mortar cured at an ambient temperature reached the compressive strength of 62 MPa and flexural strength 11.6 MPa at the age of 28 days. Compressive and flexural strengths of geopolymer mortar cured at 60 or 80 °C, respectively, reached their final values just 24 h after mixing and exceeded the values observed for samples cured at an ambient temperature three times over. However, the rapid setting prevented the mixture from the formation of a more compact and tough structure. Hence the compressive strength in 28 days was 10 MPa lower compared to that of the reference mortar. On the contrary, the mixture that was cured at decreased temperature exhibited delayed strength development, reaching the target value of 62 MPa in 28 days after mixing.

Rovnanik³⁶ found that the explanation of this behavior in geopolymer is thought to be similar to the influence of temperature on the strength development of Portland cement. At early ages, the strength increased with the temperature since at higher temperatures the geopolymerization degree was higher, and therefore the amount of reaction products increased. On the other hand, at longer ages, when the geopolymerization degree was approximately the same, the quality of reaction products was the predominant parameter. The geopolymer developed at lower temperature grew slowly and then its quality was better in terms of lower porosity and higher toughness.

Rovnanik³⁶ also found that the flexural strengths of specimens cured at different temperatures showed the same trend as for the compressive strengths. Longer curing of geopolymer mixture accelerated the development of strength in the first 24 h of hardening. Meanwhile the 1-day compressive strength of geopolymer mortar cured for 1 h at 40 °C was only 13 MPa. The strength increased by almost three times to 37 MPa when curing was prolonged to 4 h. The final values of strengths were reached approximately in 7 days and they were comparable to those observed for reference samples cured at ambient temperature. The specimens that were cured for two or more hours at high temperature reached their final strengths in 3 days with values of about 50 MPa. In contrast, when the mixture was subjected to higher temperature just for 1 h, the trend for strength development was very similar to that observed with 4-h curing at 40 °C. In this case, the early-

age compressive strength was approximately 30 MPa, but the final strength was not decreased.

Rowles and O'Connor²⁹ found that the lower-strength GPs showed a distinct "grainy" structure: a predominantly "two-phase" arrangement comprising the inorganic polymer matrix and incompletely dissolved grains. Differences between the relative amount of grain phase apparent from SEM imaging and the chemistry derived from EDS suggested that the grains were intermediate in chemical composition between that for MK and for the fully formed inorganic polymer. The presence of a two-phase material suggested that either the curing regime and/or the particle size of the MK needed to be optimized to obtain a single-phase inorganic polymer. Optimization of the curing regime would create an environment in which all of the MK could dissolve, whereas varying the initial MK particle size might provide the maximum particle size that may be fully dissolved. The microstructures for Si:Al = 1.08, corresponding to digestion with NaOH rather than sodium silicate, were dominated by undissolved grains, indicating the need to conduct the digestion with sodium silicate solution to efficiently achieve geopolymer formation. The application of sodium silicate solution was required to drive the MK-to-geopolymer dissolution reaction. Increasing the level of silicate in solution, as indicated from the microstructure trends for an increased Si:Al ratio in the starting materials, increased the extent of MK dissolution.

High strength was also associated with a fine-grained microstructure⁵⁴. For the maximum strength sample (Si:Al = 2.5/1.29; 64 MPa), the residual grains exhibited polishing relief, indicating that the matrix was harder than the grains, which was a possible explanation for the difference in compressive strength compared with, for example, sample 2.0/1.0 (51.3 MPa). There was evidence, from the appearance of microcracking for sample 3.0/1.53 (26 MPa), that a practical upper limit may exist in respect of strength optimization by increasing the Si:Al ratio for the current preparation method. The compressive strength of the GPs increased with a slight increase in Na content above the stoichiometric amount. The variation in the compressive strength of the GPs could not be attributed solely to changes in the microstructure, as it could be shown that the chemical composition of the GP also caused changes in the compressive strength. This point was highlighted with the comparison of samples 1.5/1.0 (23.4 MPa) and 2.0/1.0 (51.3 MPa) and samples 2.5/1.53 (49 MPa) and 3.0/2.0 (19.9 MPa).

Although the microstructures of these samples were similar, their compressive strengths differed by approx. 100 %. Excessive Na would break down the polymer network by terminating Si-O-Na chains, leading to a weaker material owing to a degraded polymer network. Excess Na led to the formation of Na₂CO₃ when the material was exposed to the atmosphere, thus indicating the availability of Na⁺ ions in the material. Examination of the microstructure was of value for assessing qualitatively the extent to which grain dissolution had occurred, for examining porosity, and for looking for the development of

Na_2CO_3 . However, SEM imaging alone did not give an unequivocal indication of the likely compressive strength.

Rowles and O'Connor²⁹ provided the following insights into microchemical optimization of compressive strength: (1) Chemical composition of the starting materials did not accurately predict the chemical composition of the geopolymer matrix owing to incomplete dissolution of the starting material; (2) The ideal Na:Al molar ratio of 1.0 required for charge balance in the bonding network was observed for the matrix; (3) As the nominal Si:Al molar ratio for the final material increased, the Si:Al ratio increased steadily from the MK value, without resulting in the full dissolution of the grain.

These results underline the importance of using SEM/EDS microchemical analysis for designing chemical processing conditions for strength-optimized geopolymers, rather than relying on imaging or bulk chemistry in isolation. The conclusions deduced were that: (1) The overall elemental composition of the starting materials does not accurately predict the microchemical composition of the geopolymer matrix. Whereas the material with maximum compressive strength (65 MPa) had a stoichiometric composition of $\text{Na}_n[-(\text{SiO}_2)_{2.6}(\text{AlO}_2)-]_n$, the composition of the matrix from EDS analysis was $\text{Na}_n[-(\text{SiO}_2)_{3.2}(\text{AlO}_2)-]_n$. (2) Exceeding the Si:Al ratio of strength optimization results in the development of microcracking, which substantially weakened the material. (3) The ideal Na:Al ratio of unity required for charge balance in the bonding network, for the current sample preparation method, was observed for the matrix whereas the prior study indicated that an excess of Na^+ , amounting to Na:Al = 1.25 in the starting materials, was required for formation of the optimum strength material. This is inconsistent with detailed studies by Rüscher *et al.*⁵⁵. (4) As the nominal Si:Al ratio for the final material increases, the Si:Al ratio increases steadily from the ideal MK value of unity. (5) To produce an optimum GP using the processing conditions described here, it is most likely that the particle size of the initial MK precursor would have to be reduced. (6) The lack of change in the microstructures for the Si:Al = 1.08 samples suggested the possibility that the presence of Si species in the activating solution is required to initiate polymerization.

In Zhang *et al.*³³ potassium-MK based GP average bending and compressive strengths were 5.4 and 50 MPa, respectively. The MK-based geopolymers showed the typical microstructure of a dense and homogeneous gel. The dense gel exhibited fewer cracks, mainly resulting from previous strength tests that were carried out on these specimens. Although a few unreacted particles could be observed on the surface, the geopolymerization reaction was almost complete in this group of geopolymers. From the SEM images of MK-based geopolymers at high magnification, MK-based geopolymers appeared as a flake-like layer structure similar to that of metakaolin particulates. This should not have been since the geopolymer microstructure should consist of nanoprecipitates. The flake-like layer could have been due to unreacted metakaolin sheets, as has been observed with TEM¹⁷.

Zhu *et al.*³² reported that the geopolymer binder at the air curing (AC) conditions achieved 60 MPa after 7 days, 90 % of the 28-day strength (67 MPa). After being put at 80 °C, the specimens gained higher strength in the first 7 days (69, 77 MPa) but lost strength at 28 days (46, 67 MPa). The rapid strength development is a unique property of metakaolin-based geopolymers, which has been observed in many studies^{56–57}. The elevated temperature can accelerate the geopolymerization in the first days, but longer curing at high temperatures has a negative influence on the mechanical properties^{36,58}. The strength degeneration was attributed to the loss of structural water⁵⁸ and the increased porosity and pore size^{36,59}.

Zhao *et al.*³⁴ found that their metakaolin was mainly composed of zeolite-like compounds as well as small amounts of quartz and anatase, based on their characteristic diffraction peaks⁶⁰. Sodalite zeolite phase has been reported for Na-based geopolymer of the composition $\text{Na}_2\text{O} \cdot \text{Al}_2\text{O}_3 \cdot 2\text{SiO}_2 \cdot \text{H}_2\text{O}$, as seen with *in situ*, pair distribution diffraction (PDF) synchrotron studies of geopolymer⁴³. The diffractions of zeolite-like compounds seemed to disappear with increasing the Si/Al molar ratio up to 2/1, and the resulting geopolymer only exhibited a broad hump at $2\theta = 25 - 28^\circ$ in the XRD pattern along with very small superimposed peaks for a trace of quartz impurity, indicating the completion of geopolymerization in this formulation. The unreinforced geopolymer presented a low flexural strength of 4.26 MPa. It was observed that the incorporation of polyacetal (POM) fibers imparted to the geopolymeric composites a significant improvement in flexural strength.

The flexural strength was also found to depend on fiber content and fiber length. When the POM fibers having a length of 3 mm were added into the geopolymer, the flexural strength increased with increasing the fiber content, and it achieved a maximum value at a fiber content of 1.2 wt%. Beyond that, the flexural strength presented a decrease with further increase of fiber content. However, the reinforcement effect seemed to be more significant for the geopolymeric composites with fibers having lengths of 6 and 9 mm, and the maximum flexural strength was obtained at a fiber content of 0.8 wt%.

Similar to flexural strength, the compressive strength also achieved a remarkable enhancement owing to the incorporation of POM fibers. Moreover, the compressive strength showed a similar dependence on fiber content and fiber length as the flexural strength. With increasing fiber content, the compressive strength was observed to increase continuously and then to reach a maximum value at a fiber content of 1.2 wt% for the fibers with a length of 3 mm. As for the POM fibers having lengths of 6 and 9 mm, the composites gained maximum compressive strength only at a fiber content of 0.8 wt%. Compared to unreinforced geopolymer, the flexural strength of geopolymeric composites increased by 153.7 % and 140.1 % at the optimum fiber content for the POM fibers having lengths of 6 and 9 mm, respectively. Meanwhile, the compressive strength also reached the optimal increments of 25.7 % and 24.1 % for the fibers having lengths of 6 and 9 mm, respectively.

Zhao *et al.*³⁴ concluded that compared to unreinforced geopolymer, the composites could obtain a maximum upgrade by approximately 50 % in flexural strength and by almost 26 % in compressive strength through optimization in respect of the content and length of POM fibers. The longer POM fibers generated a better reinforcement effect in the geopolymer and also imparted the composites with a lower optimal fiber content with which to achieve the maximum mechanical properties. The reinforcing behaviors of POM fibers were derived from a cumulative energy-dissipating effect by the fiber pullout and orientation, fiber rupture, fiber debonding from the matrix, and fiber bridging within cracks.

Several studies indicated that the reinforcement effect of organic fibers on geopolymers was derived from the fiber-bridging behavior (general case)^{23–24, 39, 53, 61–62}. This could be attributed to the higher numbers of fibers in cracked sections, which led to the higher fiber-bridging capacity. In addition, the longer fiber lengths favored the formation of fiber bridging among the cracks in geopolymeric composites of the same fiber content, and so was more beneficial to the reinforcing effectiveness of POM fibers.

It is considered difficult to blend flexible organic fibers discretely into the geopolymeric matrix when their concentration is excessive, because the excessive fibers may become entangled with each other in some parts of the matrix under the mechanical agitation. The fiber agglomeration occurring in the matrix can constitute an obstacle to the bonding between the matrix and fibers. Therefore, a threshold has been observed in many inorganic composites containing reinforcing organic fibers. With increasing fiber content over such a threshold, the mechanical strength shows an overall tendency to decrease. The geopolymeric composites containing the POM fibers having lengths of 6 and 9 mm have a lower threshold than those having a length of 3 mm, indicating that the longer fibers become more easily entangled with each other in the matrix. The reinforcement mechanisms of plastic fibers in cementitious materials have been extensively studied, and it is widely accepted that fiber rupture, fiber pullout, and fiber debonding from the matrix can effectively absorb and dissipate fracture energy to stabilize the propagation of cracks within the matrix when bending or compressive failure occurs in fiber-reinforced cementitious materials⁶³.

Wang *et al.*⁶⁴ investigated the effects of the concentration of the alkali activator solution and drying time on the compressive and flexural strength in a sodium-activated metakaolin system. For a 12 M NaOH activator solution, the authors reported a flexural strength > 50 MPa after 7 days and a corresponding compressive strength of ~65 MPa. Although the lengths of the specimens used by Lin *et al.*³¹ and He *et al.*⁶⁵ were also relatively small, the width and thickness were smaller, too. While the use of such small specimens is relatively common for the flexural strength testing of engineering ceramics, their applicability for geopolymers seems challenging owing to the fragility and relatively low mechanical strength of geopolymers compared to engineering ceramics. Nonetheless, unlike the flexural strength reported by Wang *et al.*⁶⁴, the mea-

surements conducted by Lin *et al.*³¹ and He *et al.*⁶⁵ seemed to obtain reasonable results.

On the other hand, the comparison of the mechanical properties of Lin *et al.*³¹ with Kriven *et al.*¹⁷ revealed major differences. The chemical composition of the geopolymers used by Kriven *et al.*¹⁷ and Lin *et al.*³¹ were identical. These compositions were close to what is widely considered to be the optimum compositional range for strong geopolymers. Although there is no general relationship between the compressive and flexural strength of geopolymers, a roughly similar compressive strength would also be expected. Given the similarity in the chemical compositions, similar properties would also be expected for the geopolymer used by Kriven *et al.*¹⁷. However, the comparison of the strength values reveals major differences. There are many factors that can affect the mechanical properties such as the material system, processing and testing parameters.

Possible explanations for the comparatively low strength values of Kriven *et al.*¹⁷ must be considered. The first possibility is that the low mechanical strength is a result of insufficient processing of the geopolymer binder. This argument is supported by the observation within the same publication that by improving the general processing and the application of a vacuum method to remove entrapped air, the compressive strength could be improved up to a maximum value of 83 MPa. This clearly highlights the effect of the processing methods on the mechanical properties. Thus, there is suspicion that the low strength values reported by Kriven *et al.*¹⁷ could be based on the measurement of in some way not visible defective specimens. In this context, the study by Kriven *et al.*¹⁷ is merely an example and the same considerations may also apply to many other studies.

He *et al.*⁶⁵ reported a flexural strength and elastic modulus of 133 MPa and 37 GPa, respectively, for a unidirectional-carbon-fiber-reinforced composite with a fiber volume content of 20–25 %. The need for standardized testing methods for geopolymer matrix composites should be emphasized. A minimum span/depth (s/d) ratio of 32:1 is recommended for the flexural testing of geopolymer matrix composites to reduce shear stresses and achieve tensile failure. Smaller s/d ratios tend to induce predominantly shear failure. Failure seems to occur owing to matrix fragmentation in the interlaminar areas of the composite despite their orientation parallel to the loading direction. The matrix is the failure-dominating component under both loading directions for the carbon composites. Given the weak nature of the geopolymer matrix, the weak matrix composite concept (weak matrix mechanical properties and weak fiber/matrix interface bonding strength) seems much more applicable to describe the behavior of geopolymer composites.

Villaquirán-Cañedo and Gutiérrez³⁷ revealed that, in general, a decrease in strength occurs at long curing ages (7-days, 41 MPa; 28-days, 42 MPa; 90-days, 38 MPa; 180-days, 24 MPa). This effect was attributed to the curing temperature and time used in the geopolymer synthesis during the initial hardening phase at 70 °C for 20 h⁶⁶. On the surface of geopolymer, at a curing age of 28 days, it was

possible to observe in the SEM micrographs small particles of unreacted residual MK embedded in the hardened gel. After 180 days, a similar morphology was observed for geopolymer, with the presence of pores and particles of unreacted MK. The greater porosity can be attributed to the effect of curing at 70 °C, and the greater amount of water in the mixture (liquid/solid molar ratio of 0.4). Although higher water contents are necessary for workability and mobilization of the alkaline ions during the mixing process, and in the fresh state, at a greater age, this contributes to contraction and cracking and increases porosity in the microstructure of the hardened gel^{66–67}.

Conflicting results on the compressive strength of fiber-reinforced geopolymer composites (FRGPCs) have been reported in the literature. In another study, an improvement in the early-age compressive strength of a PP-fiber-reinforced FRGPC was reported compared to an unreinforced one⁶¹. The source materials in this study were a combination of fly ash and calcined kaolin with a ratio of 1:2. An increase in compressive strength by about 68 % and 20 % at 1 and 3 d, respectively, was observed for a FRGC containing 0.5 wt% PP fiber. However, beyond this fiber content the compressive strength decreased at both ages.

Like cement-based fiber composites, the tensile and flexural strengths of FRGPCs are also increased with the addition of fibers. Zhang *et al.*⁶¹ studied the early-age flexural strength of PP-fiber FRGPCs. A significant improvement in the flexural strength of the PP-fiber FRGPCs at 1 and 3 days was observed. The flexural strength almost doubled with the addition of 0.75 % PP fiber at both ages.

In another study, Natali *et al.*⁶⁸ studied the flexural behavior of metakaolin/slag-based FRGPCs containing four different types of fiber. The fibers used were carbon, E-glass, polyvinyl alcohol (PVA) and polyvinyl chloride (PVC). Each of the types of fiber improved the flexural strength of the FRGPCs. Most notably, carbon- and PVA-fiber-reinforced FRGPCs exhibited about a 50 % and 62 % increase in flexural strength, respectively, along with a significant improvement in post-crack ductility. The carbon FRGPC also had the highest toughness index of all the FRGPCs.

In another study, the flexural behavior of FRGPCs with extruded PVA fibers made from a sodium silicate/sodium hydroxide activated metakaolin and a fly ash/metakaolin blend were investigated^{68–69}. The PVA fibers (14 µm in diameter, 6 mm in length) were at 0 vol%, 1 vol% and 2 vol% in the composite and the composite was produced using a single-screw extruder. The samples were allowed to cure at room temperature and the flexural strength was tested after 28 days. In the flexural tests, the metakaolin-based FRGPC exhibited substantial increases in mid-point deflection and distributed microcracking with an increase in fiber content. However, the ultimate flexural strength was not improved with the addition of PVA fibers to the metakaolin-based FRGPC. On the other hand, increasing the quantity of fly ash in the metakaolin/fly ash-blended FRGPC decreased the flexural strength except for the composite containing 10 % fly ash, where the flexural strength increased by about 30 % compared to the com-

posite containing no fly ash (i.e. 100 % metakaolin). The decrease in flexural strength could be due to the lower reactivity of fly ash compared to metakaolin, which caused a ‘dilution’ of the strength-bearing phases. This was also observed during analysis of the failure mechanism, which varied from fiber fracture (low fly ash) to fiber pull-out (high fly ash), because of the weakening of the matrix due to reduced geopolymer formation, which altered the fiber/matrix bonding. In this system, fly ash was shown to play a complex role in the metakaolin/fly-ash-blended geopolymeric composites⁵⁴.

The poly(acetal) POM fiber used in the paper by Zhao *et al.*³⁴ was still in the development phase. It has not been commercialized so far. According to the authors, POM is one of the most important engineering thermoplastics. The addition of 1 wt% POM fiber to a poly(sialate-siloxo) geopolymer provided higher strength associated with a new property: low friction coefficient. The mechanical and tribological properties of the resulting composites were evaluated, and the morphology and microstructure were investigated. The POM fibers provided significant mechanical reinforcement for the metakaolin-based geopolymer. The composites were optimized for flexural and compressive strength in respect of 1 wt% fiber content and 6 mm fiber length. Compared to unreinforced geopolymer, the composites obtained an optimum improvement in flexural strength up to 11 MPa compared to 4.5 MPa for plain geopolymer, and a compressive strength up to 62 MPa compared to 49 MPa. The POM geopolymer also achieved a considerable reduction in the friction coefficient and abrasion loss rate. Such an enhancement of tribological performance was ascribed to the formation of self-lubricating transfer films between the contact surfaces of composites against the steel counterpart. According to the authors, the improved mechanical strength, enhanced tribological properties, environmental friendliness and relatively low cost made these developed POM geopolymeric composites potentially attractive for a number of construction and civil engineering applications.

Alzeer and MacKenzie⁴⁸ reported the use of two types of wool (carpet wool and Merino wool) for this purpose, with the aim of producing novel, environment-friendly low-cost composites with improved flexural strength and graceful failure for engineering and construction applications. The mechanical properties of fiber-reinforced composites depend on the fiber-matrix interface, since the strength of such a composite is obtained by transferring the stress between the fibers and the matrix. With an average 5-wt% wool fiber content, the flexural strengths were in the range of 8.1 to 9.1 MPa, compared with 5.8 MPa for the pure geopolymer, and graceful failure, unlike the unreinforced matrix that displayed ceramic-like brittle fracture.

Alzeer and MacKenzie⁷⁰ studied another bio-fiber, flax. A poly(sialate-siloxo) geopolymer was unidirectionally reinforced with 4–10 vol% natural cellulose-based fiber, flax *phormium tenax*. The mechanical properties of the fiber-reinforced composites improved with increasing fiber content, achieving ultimate flexural strengths of about 70 MPa at 10 vol% fiber contents. This repre-

sented a significant improvement on the flexural strength of the unreinforced geopolymer matrix (about 5.8 MPa). The composites showed graceful failure, unlike the brittle failure of the matrix. The results of scanning electron microscopy, combined with thermogravimetric analysis (TGA) and thermal shrinkage measurements of these composites suggested that despite the formation of microcracks due to water loss from the geopolymer matrix, the fibers were thermally protected by the matrix up to 400 °C. The flax fibers did not appear to be compromised by the alkaline environment of the matrix, suggesting new possible applications for these low-cost simply prepared construction materials.

IV. Conclusions

The general observations from the reviewed worldwide research on MK-based GPCs reveal a broad range of processing, testing parameters and results:

1. Metakaolin (MK) has the main components SiO_2 and Al_2O_3 in weight percentages ranging from 44.4–73 % and 14.5–47.43 %, respectively.
2. MK calcination temperatures and holding time ranged from 650–900 °C and 0.5–24 h, respectively.
3. GP processing mixing speeds and times ranged from 600–2500 rpm and 3–30 min, respectively.
4. Geopolymer Si/Al ratios ranged from 1.4–8.
5. Compressive strength testing samples were either cylindrical (3–50 mm diameter) or cubic (20–50 mm).
6. Compressive strength testing number of samples ranged from 3–20.
7. Compressive strength testing speeds ranged from 0.0001–0.0833 mm/s.
8. GP density ranged from 1.34–2.31 g/cm³.
9. The compressive strengths (1, 3, 7, 14 and 28 d) lay in the broad range 13.9–109 MPa.
10. Flexural strength testing methods were either 4-point or 3-point loading.
11. The 4-point flexural strength testing samples' dimensions ranged from 40–150 mm (length), 1.5–25 mm (depth) and 10–28 mm (breadth).
12. The 4-point flexural strength testing number of samples ranged from 5–6.
13. The 4-point flexural strength testing speed was 0.001 mm/s.
14. GPC density ranged from 1.47–1.51 g/cm³.
15. The 4-point flexural strengths (7 d) lie in the broad range 2.8–14.1 MPa.
16. The 3-point flexural strength testing samples' dimensions ranged from 30–160 mm (length), 4–40 mm (depth) and 3–40 mm (breadth).
17. The 3-point flexural strength testing number of samples ranged from 3–7.
18. The 3-point flexural strength testing speed ranged from 0.005–0.010 mm/s.
19. The 3-point flexural strengths (1, 3, 7, 14 and 28 d) lay in the broad range 3.1–16.8 MPa.

The worldwide investigations on MK-based particles and fiber-reinforced GPC reviewed here revealed large variations of data results among and within different laboratories. Due to the unavailability of a standard for

processing and testing geopolymer composites, different laboratories use differing procedures, making data comparison very difficult. The promising market of geopolymer composites for the sustainable construction industry would benefit from a uniform standard for laboratory processing and testing. This would contribute to the creation of a larger and more reliable data bank, so as to lead to the manufacture and certification of geopolymeric sustainable construction materials.

References

- 1 Duxson, P., Provis, J.L., Lukey, G.C., Mallicoat, S.W., Kriven, W.M., van Deventer, J.S.J.: Understanding the relationship between geopolymer composition, microstructure and mechanical properties, *Colloid. Surface. A*, **269**, 47–58, (2005). doi: 10.1016/j.colsurfa.2005.06.060
- 2 Görhan, G., Aslaner, R., Sinik, O.: The effect of curing on the properties of metakaolin and fly ash-based geopolymer paste, *Compos. Part B-Eng.*, **97**, 329–335, (2016).
- 3 Hussain, M., Varely, R., Cheng, Y.B., Mathys, Z., Simon, G.P.: Synthesis and thermal behavior of inorganic-organic hybrid geopolymer composites, *J. Appl. Polym. Sci.*, **96**, 112–121, (2005).
- 4 Heah, C.Y., Kamarudin, H., Mustafa Al Bakri, A.M., Binhusain, M., Luqman, M., Khairul Nizar, I., Ruzaid, C.M., Liew, Y.M.: Effect of curing profile on Kaolin-based geopolymers, *Phys. Proc.*, **22**, 305–311, (2011).
- 5 Davidovits, J.: 30 years of success and failures in geopolymer applications – market trends and potential breakthroughs. In: Geopolymer 2002 Conference Keynotes, October 28–29, Melbourne, Australia, 1–15, 2002.
- 6 Kriven, W.M.: Inorganic polysialates or “geopolymers”, *Am. Ceram. Soc. Bull.*, **89**, [4], 31–34, (2010).
- 7 Kriven, W.M.: Geopolymer-based composites. In: *Ceramics and Carbon Matrix Composites*, Vol 5, edited by Marina RugglesWrenn. Part of an 8-Volume set of books entitled *Comprehensive Composite Materials II*, Peter Beaumont and Carl Zweben, Co-editors-in-chief. Published by Elsevier, Oxford, UK, in press 2017.
- 8 Davidovits, J.: Geopolymer cement to minimize carbon-dioxide greenhouse-warming. In: *Cement-based materials: Present, future and environmental aspects*, *Ceram. Trans.*, **37**, 165–182, (1993).
- 9 Davidovits, J.: Carbon-dioxide greenhouse-warming: what future for Portland cement. In: *Emerging Technologies Symposium on Cements and Concretes in the Global Environment*, March 1993, Portland Cement Association, Chicago, Illinois, 21, 1993.
- 10 Duxson, P., Provis, J.L., Lukey, G.C., van Deventer, J.S.J.: The role of inorganic polymer technology in development of ‘green concrete’, *Cem. Concr. Res.*, **37**, 1590–7, (2007).
- 11 van Deventer, J.S.J., Provis, J.L., Duxson, P., Brice, D.G.: Chemical research and climate change as drivers in the commercial adoption of alkali activated materials, *Waste Biomass Valor.*, **1**, 145–55, (2010).
- 12 Davidovits, J.: Geopolymer cement, a review. Institut Géopolymère, St. Quentin, France, http://www.geopolymer.org/fichiers_pdf/GPCement2013.pdf, 2013.
- 13 Barbosa, V.F.F., MacKenzie, K.J.D.: Thermal behaviour of inorganic geopolymers and composites derived from sodium polysialate, *Mater. Res. Bull.*, **38**, [2], 319–31, (2003).
- 14 Duxson, P., Mallicoat, S.W., Lukey, G.C., Kriven, W.M., van Deventer, J.S.J.: The effect of alkali and Si/Al ratio on the development of mechanical properties of metakaolin-based geopolymers, *Colloid. Surface. A*, **292**, 8–20, (2007). doi: 10.1016/j.colsurfa.2006.05.044

- 15 Duxson, P., Fernández-Jiménez, A., Provis, J.L., Lukey, G.C., Palomo, A., van Deventer, J.S.J.: Geopolymer technology: the current state of the art, *J. Mater. Sci.*, **42**, 2917–2933, (2007). doi: 10.1007/s10853-006-0637-z
- 16 Vickers, L., van Riessen, A., Rickard, W.D.A.: Precursors and additives for geopolymer synthesis. In: Fire-Resistant Geopolymers - Role of Fibres and Fillers to Enhance Thermal Properties, Ch.2, Springer, 2015.
- 17 Kriven, W.M., Bell, J.L., Gordon, M.: Microstructure and microchemistry of fully-reacted geopolymers and geopolymer matrix composites, *Ceram. Trans.*, Ch15, 227–250, (2003).
- 18 Kriven, W.M., Bell, J., Gordon, M.: Geopolymer refractories for the glass manufacturing industry, *Ceram. Eng. Sci. Proc.*, **25**, [1], Ch. 5, 57–79, (2004). doi: 10.1002/9780470294857.ch5
- 19 Lizcano, M., Kim, H.S., Basu, S., Radovic, M.: Mechanical properties of sodium and potassium activated metakaolin-based geopolymers, *J. Mater. Sci.*, **47**, 2607–2616, (2012).
- 20 Rickard, W.D.A., Vickers, L., van Riessen, A.: Performance of fibre reinforced, low density metakaolin geopolymers under simulated fire conditions, *Appl. Clay Sci.*, **73**, 71–77, (2013).
- 21 Musil, S.: Novel, inorganic composites using porous, alkali-activated, aluminosilicate binders. Dissertation, University of Illinois at Urbana-Champaign, Urbana, IL, USA, 2014.
- 22 Ribero, D., Kriven, W.M.: Properties of geopolymer composites reinforced with basalt chopped strand mat or woven fabric, *J. Am. Ceram. Soc.*, 1–8, (2016). doi: 10.1111/jace.14079
- 23 Sankar, K., Sá Ribeiro, R.A., Sá Ribeiro, M.G., Kriven, W.M.: Potassium-based geopolymer composites reinforced with chopped bamboo fibers, *J. Am. Ceram. Soc.*, **100**, [1], 49–55, (2017). doi: 10.1111/jace.14542
- 24 Sá Ribeiro, R.A., Sá Ribeiro, M.G., Sankar, K., Kriven, W.M.: Bamboo-geopolymer composite: A preliminary study, in developments in strategic ceramic materials II: *Ceram. Eng. Sci. Proc.*, **37**, [7], 135–143, John Wiley & Sons, Inc., Hoboken, NJ, USA, (2017). doi: 10.1002/9781119321811.ch13
- 25 Kirschner, A.V., Harmuth, H.: Investigation of geopolymer binders with respect to their application for building materials, *Ceramics – Silikáty*, **48**, [3], 117–120, (2004).
- 26 Pouhet, R.: Formulation and durability of metakaolin-based geopolymers. Dissertation, Université de Toulouse, France, 2015.
- 27 Krivenko, P.V., Kovalchuk, G.Y.: Directed synthesis of alkaline aluminosilicate minerals in a geocement matrix, *J. Mater. Sci.*, **42**, 2944–2952, (2007).
- 28 Kong, D.L.Y., Sanjayan, J.G., Sagoe-Crentsil, K.: Factors affecting the performance of metakaolin geopolymers exposed to elevated temperatures, *J. Mater. Sci.*, **43**, 824–831, (2008).
- 29 Rowles, M.R., O'Connor, B.H.: Chemical and structural microanalysis of aluminosilicate geopolymers synthesized by sodium silicate activation of metakaolinite, *J. Am. Ceram. Soc.*, **92**, [10], 2354–2361, (2009).
- 30 Yunsheng, Z., Wei, S., Zongjin, L.: Composition design and microstructural characterization of calcined kaolin-based geopolymer cement, *Appl. Clay Sci.*, **47**, 271–275, (2010).
- 31 Lin, T., Jia, D., He, P., Wang, M., Liang, D.: Effects of fiber length on mechanical properties and fracture behavior of short carbon fiber reinforced geopolymer matrix composites, *Mater. Sci. Eng. A*, **497**, 181–185, (2008).
- 32 Zhu, H., Zhang, Z., Deng, F., Cao, Y.: The effects of phase changes on the bonding property of geopolymer to hydrated cement, *Constr. Build. Mater.*, **48**, 124–130, (2013).
- 33 Zhang, H.Y., Kodur, V., Wu, B., Cao, L., Qi, S.L.: Comparative thermal and mechanical performance of geopolymers derived from metakaolin and fly ash, *J. Mater. Civ. Eng.*, **28**, [2], 1–12, (2016).
- 34 Zhao, W., Wang, Y., Wang, X., Wu, D.: Fabrication, mechanical performance and tribological behaviors of polyacetal-fiber-reinforced metakaolin-based geopolymeric composites, *Ceram. Int.*, **42**, 6329–6341, (2016).
- 35 Kenne, B.B.D., Elimbi, A., Cyr, M., Dika, J.M., Tchakoute, H.K.: Effect of the rate of calcination of kaolin on the properties of metakaolin-based geopolymers, *J. Asian Ceram. Soc.*, **3**, 130–138, (2015).
- 36 Rovnaník, P.: Effect of curing temperature on the development of hard structure of metakaolin-based geopolymer, *Constr. Build. Mater.*, **24**, 1176–1183, (2010).
- 37 Villaquirán-Cacedo, M.A., Gutiérrez, R.M.: Synthesis of ternary geopolymers based on metakaolin, boiler slag and rice husk ash, *DYNA*, **82**, [194], 104–110, (2015).
- 38 Kabir, S.M.A., Alengaram, U.J., Jumaat, M.Z., Sharmin, A., Islam, A.: Influence of molarity and chemical composition on the development of compressive strength in POFA based geopolymer mortar, *Adv. Mater. Sci. Eng.*, **2015**, 1–15, (2015).
- 39 Sá Ribeiro, R.A., Sá Ribeiro, M.G., Sankar, K., Kriven, W.M.: Geopolymer-bamboo composite – A novel sustainable construction material, *Constr. Build. Mater.*, **123**, 501–507, (2016). doi: 10.1016/j.conbuildmat.2016.07.037
- 40 Barbosa, V.F.F., MacKenzie, K.J.D., Thaumaturgo, C.: Synthesis and characterisation of materials based on inorganic polymers of alumina and silica: Sodium polysialate polymers, *Int. J. Inorg. Mater.*, **2**, 309–317, (2000).
- 41 Abbasi, S.M., Ahmadi, H., Khalaj, G., Ghasemi, B.: Microstructure and mechanical properties of a metakaolinite-based geopolymer nanocomposite reinforced with carbon nanotubes, *Ceram. Int.*, **42**, 15171–15176, (2016).
- 42 Bell, J.L., Sarin, P., Provis, J.L., Haggerty, R.P., Driemeyer, P.E., Chupas, P.J., van Deventer, J.S.J., Kriven, W.M.: Atomic structure of a cesium aluminosilicate geopolymer: A pair distribution function study, *Chem. Mater.*, **20**, [14], 4768–4776, (2008).
- 43 Bell, J.L., Sarin, P., Driemeyer, P.E., Haggerty, R.P., Chupas, Kriven, W.M.: X-ray pair distribution function analysis of a metakaolin-based $\text{KAl-Si}_2\text{O}_6 \cdot 5.5\text{H}_2\text{O}$ inorganic polymer (geopolymer), *J. Mater. Chem.*, **18**, [48], 5974–5981, (2008).
- 44 Latella, B.A., Perera, D.S., Durce, D., Mehrtens, E.G., Davis, J.: Mechanical properties of metakaolin-based geopolymers with molar ratios of $\text{Si}/\text{Al} \approx 2$ and $\text{Na}/\text{Al} \approx 1$, *J. Mater. Sci.*, **43**, 2693–2699, (2008).
- 45 Rill, E., Lowry, D.R., Kriven, W.M.: Properties of basalt fiber reinforced geopolymer composites, in strategic materials and computational design, edited by W.M. Kriven, Y. Zhou and M. Radovic, *Cer. Eng. Sci. Proc.*, **31**, [10], 57–69, (2010).
- 46 Musil, S.S., Kutyla, G., Kriven, W.M.: The effect of basalt chopped fiber reinforcement on the mechanical properties of potassium based geopolymer, in developments in strategic materials and computational design III, edited by W.M. Kriven, A.L. gyekenyesi, G. westin and J. wang, *Cer. Eng. Sci. Proc.*, **33**, [10], 31–42, (2013).
- 47 Musil, S.S., Keane, P.F., Kriven, W.M.: Green composite: sodium-based geopolymer reinforced with chemically extracted corn husk fibers, in developments in strategic materials and computational design IV, edited by W.M. Kriven, J. wang, Y. Zhou and A.L. gyekenyesi, *Cer. Eng. Sci. Proc.*, **34**, [10], 123–133, (2014).
- 48 Alzeer, M., MacKenzie, K.J.D.: Synthesis and mechanical properties of new fibre-reinforced composites of inorganic polymers with natural wool fibres, *J. Mater. Sci.*, **47**, 6958–6965, (2012). doi: 10.1007/s10853-012-6644-3
- 49 Sankar, K., Kriven, W.M.: Sodium geopolymer reinforced with jute weave, in developments in strategic materials and computational design V, edited by W.M. Kriven, D. Zhou, K. Moon, T. Hwang, J. Wang, C. Lewinsohn and Y. Zhou, *Cer. Eng. Sci. Proc.*, **38**, [10], 39–60, (2015).

- 50 Heo, U.H., Sankar, K., Kriven, W.M., Musil, S.S.: Rice husk ash as a silica source in geopolymer formulation, in developments in strategic materials and computational design V, edited by W.M. Kriven, D. Zhou, K. Moon, T. Hwang, J. Wang, C. Lewinsohn and Y. Zhou, *Cer. Eng. Sci. Proc.*, **38**, [10], 87–102, (2015).
- 51 Sankar, K., Kriven, W.M.: Potassium geopolymer reinforced alkali-treated fique, in developments in strategic materials and computational design V, edited by W.M. Kriven, D. Zhou, K. Moon, T. Hwang, J. Wang, C. Lewinsohn and Y. Zhou, *Cer. Eng. Sci. Proc.*, **38**, [10], 61–78, (2015).
- 52 Sankar, K., Kriven, W.M.: Green composite: sodium geopolymer reinforced with malva fibers, *J. Am. Ceram. Soc.*, (in preparation), (2017).
- 53 Sá Ribeiro, R.A., Sá Ribeiro, M.G., Sankar, K., Kutyla, G.P., Kriven, W.M.: Mixed alkali regional metakaolin-based geopolymer, In: Developments in strategic ceramic materials II: *Ceram. Eng. Sci. Proc.*, **37**, [7], 123–133, John Wiley & Sons, Inc., Hoboken, NJ, USA, (2017). doi: 10.1002/9781119321811.ch12
- 54 Zhang, Y., Sun, W., Li, Z., Zhou, X.: Geopolymer extruded composites with incorporated fly ash and polyvinyl alcohol short fiber, *ACI Mater. J.*, **106**, [1], 3–10, (2009).
- 55 Rüscher, C.H., Mielcarek, E., Lutz, W., Ritzmann, A., Kriven, W.M.: Weakening of alkali-activated metakaolin during aging investigated by the molybdate method and infrared absorption spectroscopy, *J. Am. Ceram. Soc.*, **93**, [9], 2585–2590, (2010).
- 56 Zhang, Z., Yao, X., Zhu, H.: Potential application of geopolymers as protection coatings for marine concrete I. basic properties, *Appl. Clay Sci.*, **49**, 1–6, (2010).
- 57 Lloyd, R.R.: Accelerated ageing of geopolymers, in Provis, Van Deventer, editors. *Geopolymers: Structure, processing, properties and industrial applications*. CRC Press, 139–166, (2009).
- 58 Zhang, Z., Yao, X., Zhu, H., Chen, Y.: Role of water in the synthesis of calcined kaolin-based geopolymer, *Appl. Clay Sci.*, **43**, 218–223, (2009).
- 59 Muñoz-Villarreal, M.S., Manzano-Ramírez, A., Sampieri-Bulbarela, S., Gasca-Tirado, J.R., Reyes-Araiza, J.L., Rubio-Avalos, J.C., et al.: The effect of temperature on the geopolymerization process of a metakaolin-based geopolymer, *Mater. Lett.*, **65**, [6], 995–998, (2011).
- 60 Rasouli, H.R., Golestani-fard, F., Mirhabibi, A.R., Nasab, G.M., Mackenzie, K.J.D., Shahraki, M.H.: Fabrication and properties of microporous metakaolin-based geopolymer bodies with polylactic acid (PLA) fibers as pore generators, *Ceram. Int.*, **41**, 7872–7880, (2015).
- 61 Zhang, Z., Yao, X., Zhu, H., Hua, S.: Preparation and mechanical properties of polypropylene fiber reinforced calcined kaolin-fly ash based geopolymer, *J. Cent. South. Univ. T.*, **16**, 49–52, (2009).
- 62 Zhang, Y., Li, S., Xu, D., Wang, B., Xu, G., Yang, D., Wang, N., Liu, H., Wang, Y.: A novel method for preparation of organic resins reinforced geopolymer composites, *J. Mater. Sci.*, **45**, 1189–1192, (2010).
- 63 Yin, S., Tuladhar, R., Shi, F., Combe, M., Collister, T., Sivakugan, N.: Use of macro plastic fibers in concrete: A review, *Constr. Build. Mater.*, **93**, 180–188, (2015).
- 64 Wang, H., Li, H., Yan, F.: Synthesis and mechanical properties of metakaolinite-based geopolymer, *Colloid Surface A*, **268**, 1–6, (2005).
- 65 He, P., Jia, D., Lin, T., Wang, M., Zhou, Y.: Effects of high-temperature heat treatment on the mechanical properties of unidirectional carbon fibre reinforced geopolymer composites, *Ceram. Int.*, **36**, 1447–1453, (2010).
- 66 Rashad, A.M.: Alkali-activated metakaolin: A short guide for civil engineer – an overview, *Constr. Build. Mater.*, **41**, 751–765, (2013).
- 67 Arellano-Aguilar, R., Burciaga-Díaz, O., Gorokhovskiy, A., Escalante-García, J.I.: Geopolymer mortars based on a low grade metakaolin: effects of the chemical composition, temperature and aggregate-binder ratio, *Constr. Build. Mater.*, **50**, 642–648, (2014).
- 68 Natali, A., Manzi, S., Bignozzi, M.C.: Novel fiber reinforced composite materials based on sustainable geopolymer matrix, *Procedia Engineering*, **21**, 1124–31, (2011).
- 69 Li, Z., Zhang, Y., Zhou, X.: Short fibre reinforced geopolymer composites manufactured by extrusion, *J. Mater. Civil Eng.*, **17**, [6], 624–31, (2005).
- 70 Alzeer, M., MacKenzie, K.J.D.: Synthesis and mechanical properties of novel composites of inorganic polymers (geopolymers) with unidirectional natural flax fibers (phormium tenax), *Appl. Clay Sci.*, **75**–**76**, 148–152, (2013).
- 71 Sá Ribeiro, R.A., Kutyla, G.P., Sá Ribeiro, M.G., Kriven, W.M.: Amazonian metakaolin reactivity for geopolymer synthesis, *Cement Concrete Comp.*, unpublished, (2017).
- 72 Cho, S.: Geopolymer composites and their applications in stress wave mitigation. Dissertation, University of Illinois at Urbana-Champaign, USA, 2015.

